Brillouin and Rayleigh scattering studies of the phase transition in chloranil

A. Yoshihara, E. R. Bernstein, and J. C. Raich

A. Yoshihara, E. R. Bernstein, and J. C. Raich

Brillouin and Rayleigh scattering studies of the phase transition in chloranil[a)]

A. Yoshihara, E. R. Bernstein, and J. C. Raich

Department of Chemistry, Department of Physics, Colorado State University, Fort Collins, Colorado 80523
(Received 3 February 1983; accepted 25 March 1983)

The nonferroic (constant rotational symmetry) phase transition at $\sim$93 K in chloranil ($C_6Cl_4O_2$) is investigated by Brillouin and Rayleigh light scattering. The phase transition is driven by a zone boundary soft mode at the (00 1/2) point which, through various coupling mechanisms, can affect the zone center strains. The major conclusions of these investigations are: (1) the LA-phonon mode propagating along the [010*] direction exhibits a step function anomaly at T_c with an associated transition region in the low temperature phase and a linewidth anomaly. The frequency of this LA mode in the transition region decreases below its low temperature phase value near T_c; (2) the lowest frequency QTA phonon propagating around [010*] has a negative temperature coefficient in the high temperature phase which goes to zero in the low temperature phase; (3) external stress induced relaxation processes can be observed by correlation scattering spectroscopy which are highly polarization, experimental scattering geometry, and stress direction dependent; (4) the relaxation time and intensity of scattered light behave anomalously in the vicinity of the phase transition; and (5) a similar intensity anomaly without a relaxation time anomaly is observed in the absence of external stress applied to the sample. These data are analyzed using a theory developed by Yao, Cummins, and Bruce for improper ferroelastic–ferroelectric phase transitions. The negative temperature slope of the QTA mode in the high temperature phase is thought to be associated with an incipient, unrealized phase instability driven by an optical mode at 16 cm^{-1} with similar temperature dependence.

I. INTRODUCTION

Chloranil, $C_6Cl_4O_2$, has a monoclinic structure at room temperature $[C_{2h}^5\text{-}P2_1/a\ (Z=2)]^1$ and exhibits a second order structural phase transition at $\sim$93 K. The low temperature crystal structure is also monoclinic with space group $C_{2h}^5\text{-}P2_1/n\ (Z=4)$.[2–4] Chloranil is one of the rare examples of a molecular crystal exhibiting a second order phase transition driven by a Brillouin zone boundary rotational soft optical phonon. The wave vector involved corresponds to the point $(0,0,\frac{1}{2})$ in the zone.[5] The phase transition has been confirmed by means of ^{35}Cl NQR and Zeeman effect measurements by Richardson.[2] These experiments suggest that the transition is a zone boundary one and related to molecular rotations around an axis perpendicular to the molecular plane. Hanson[6] observed a restoring mode in the low temperature phase by Raman scattering and confirmed that the phase transition is induced by a soft zone boundary optical phonon.

Chloranil turns out to be a model system for the study of phase transitions in molecular crystals and has been investigated by a number of different techniques. Among these are NQR,[3,7–9] specific heat measurements,[4] Raman scattering,[6,10–14] Brillouin scattering,[15] infrared spectroscopy,[5,16–18] neutron inelastic scattering,[19(a)] neutron elastic scattering,[19(b)] and dilatometry.[13]

As indicated above, the rotational symmetry of the chloranil crystal does not change at the phase transition (C_{2h}^5) but the translational symmetry is broken. Thus, this transition is an example of a "nonferroic" one.[20]

Terauchi et al.[5] observed superlattice reflections at positions $(hkl+\frac{1}{2})$ in x-ray scattering for the low temperature phase and also found that the intensities can be accounted for by small amplitude molecular rotations about an axis perpendicular to the molecular plane. Recent x-ray analysis[18] reveals, in addition, that the molecules also rotate around the C=O bond axis. These two rotational degrees of freedom, taken in linear combination, can be considered to be the order parameter for the chloranil phase transition. These authors also reported diffusion x-ray scattering in the high temperature phase, the intensity of which diverges following a mean field behavior, $I \sim (\omega_s^2)^{-1} \sim (T-T_c)^{-1}$.

Raman scattering experiments[13] also portray a mean fieldlike behavior for the soft mode frequency in the low temperature phase, $\omega_s^2 \sim (T_c - T)$. Such behavior has been confirmed by more extensive studies entailing pressure dependences of the soft mode and phase diagrams: it was found that $dT_c/dP = 7.5$ K/kbar and $\omega_s^2 \sim (p - p_c)$ in which $p_c = 440$ bar at $T = 97$ K.[14] These x-ray and Raman studies are noteworthy here because they emphasize a mean fieldlike behavior for the soft mode in both high and low temperature phases. These results, moreover, are in substantial agreement with neutron inelastic scattering studies of the squared soft mode frequency.[19] The completely classical results for the soft mode frequency in the high temperature phase are $\omega_s^2 \sim 0.0082$ (meV^2/K) $(T-92)$ $[95 \le T \le 270$ K$]$. In the low temperature phase agreement between the Raman and neutron data is also quite good.

On the other hand, a neutron inelastic scattering experiment[19] reported that intensity at $(-1,0,3.5)$ and $(1,0,2.5)$ obeys a power law $(T_c - T)^\beta$ with $\beta = 0.33 \pm 0.02$ in the temperature range $0.005 < (1 - T/T_c) < 0.05$ in the low temperature phase. This suggests the

order parameter also follows the same law. Recent x-ray structural analysis[18] obtained similar temperature dependences for the molecular rotation angles which can be considered to the order parameter for the transition. The critical index β is again nonclassical. Recent neutron elastic scattering studies of temperature and pressure dependence of the order parameter also support these results.[19(b)] The critical index for the correlation length has been determined by neutron scattering as well and is given by

$$\xi \sim (1 - T_c/T)^{\nu} \ ; \quad \nu = 0.62 \pm 0.04 \ .$$

These indices ν and β are very close to the theoretical results of renormalization group theory for a three-dimensional Ising model ($\beta = 0.315$ and $\nu = 0.643$). Similar indices have been found for the structural phase transition in $SrTiO_3$.[21] There is no particular reason to expect an equality between the indices for ω_s and ξ or η (order parameter); such equalities only hold in classical mean field (Landau) theories. One can thus anticipate nonmean field behavior around the transition temperature.

In addition to the soft rotational mode response observed in the neutron scattering experiments, this technique has been able to characterize a central peak for chloranil. The central peak intensity begins to grow around 140 K, $T_c + 50$ K, and dramatically increases as temperature approaches the transition temperature. The width of the central peak is less than 0.9 μeV and could not be resolved. This observation is, to the best of our knowledge, the first clear cut observation of a central peak in a molecular crystal.

Since the discovery of a central peak in $SrTiO_3$ by neutron inelastic scattering[22] the phenomenon has drawn a good deal of interest and attention. Similar critical behavior has now been observed at many other structural phase transitions (e.g., KH_2PO_4,[23] $KH_3(SeO_3)_2$,[24] and $KMnF_3$[25]). KH_2PO_4 (KDP) is the system for which the most extensive studies of central peak phenomena have been reported. Three types of central peaks have been observed in KDP through Brillouin scattering techniques[26,27]: (1) a central peak due to static defects in the crystal which can be annealed away. The divergence of this intensity is not well expressed by a simple power law except in the mean-field limit of Halperin and Varma[28]; (2) a central peak observable only after the first has been removed through annealing. The divergence of this feature obeys a mean-field expectation, $(T - T_c)^{-1}$. The origin of this central peak is not as yet clarified[27]; and (3) a central peak observable only in the low temperature phase and in the narrow range about 0.1 K below T_c.[26] This central peak is assigned to be associated with the heat diffusion (entropy) mode–order parameter interaction, allowed only in the low temperature phase due to symmetry differences of these two properties in the high temperature phase. If this later interaction becomes allowed in the high temperature phase through the application of a symmetry breaking electric field, it is still found that a central peak cannot be associated with this mechanism in the high temperature phase. This observation suggests that the temperature dependence of the order parameter, which is

very steep in KDP near T_c, is an important parameter for this particular central peak.[26,27] Unfortunately, the origin of the central peaks in other systems has not been so extensively studied and established to date.[29] Several theoretical models based on defect dynamics,[28] microdomain motion,[30] the heat diffusion mode,[31] phonon density fluctuations,[32] and solitons[33] have been proposed to explain central peak phenomena.

Previous Brillouin scattering experiments on chloranil[15] have revealed a large step function anomaly at T_c (~ 93 K) in the Brillouin frequency as a function of temperature. In addition, anomalous line width behavior has also been characterized for this same mode, a quasilongitudinal acoustic phonon which propagates along the reciprocal a direction, a^*. The magnitude of this step is about 17% of the room temperature frequency of this mode. Similar elastic anomalies have been observed in Brillouin scattering in triglycine sulfate $(TGS)^{34}$ and thiourea[35] around their second order phase transition temperatures.

The order parameter for the chloranil nonferroic phase transition can be considered to be a linear combination of molecular rotations about an axis perpendicular to the molecular plane and molecular rotations about the $C=O$ axis. This motion belongs to a one-dimensional irreducible representation of the space group at the point $(0, 0, \frac{1}{2})$. At this point on the zone boundary, the star of the wave vector has only one arm and is nondegenerate.[36] Possible couplings between the order parameter and the zone center strains can be represented by

$$F_{e,\eta} = -\frac{1}{2}(Ke_1 + Je_2 + Le_3 + Me_5 + Ne_4^2 + Pe_6^2)\eta^2$$

in which η denotes the order parameter and $e_i (i = 1, \ldots, 6)$ are the zone center strains. This form of interaction would predict no soft zone center phonon modes. Applying the Landau theory to this coupling term,[37] step function anomalies can be anticipated for elastic constants c_{11}, c_{22}, c_{33}, and c_{55}. On the other hand, elastic constants c_{44} and c_{66} are expected to change their slopes at the transition temperature in a continuous fashion. These features have not been fully established yet by the previous Brillouin work.

In a series of studies of the phase transitions in molecular crystals (e.g., benzil,[38] s-triazine,[39] and urea[40]) by Brillouin and correlation scattering techniques, an intensity autocorrelation function could be observed in benzil and urea but not in s-triazine when an external periodic stress pulse was applied to the sample. Relaxation times and photon counting rates exhibit an anomalous increase around the transition temperature in benzil; these anomalies could be removed by annealing. The observed anomalies are similar in many respects to central peak phenomena even though they are associated with the external stress pulse and thus not actually "intrinsic" lattice dynamical effects. To explain such observations in benzil, a phenomenological approach based on the theory of anelastic solids has been developed and applied successfully.

In urea, for which no phase transition could be detected, a correlation function was observed but without

anomalous behavior. In triazine and NH_4Cl^{38-40} no cor-
relation function is observed at any temperature inde-
pendent of the external applied stress conditions. It is
thereby demonstrated, experimentally and theoretically,
that there is a close correlation between modulated
(driven) defect dynamics and the underlying lattice dy-
namics, especially near a critical point or phase transi-
tion. Indeed, coupling between defects and the phonon
and fluctuation spectra of the lattice controls the be-
havior of the defects.

In this report, new Brillouin scattering and correla-
tion spectroscopy results are reported for chloranil and
in particular, the phase transition at 93 K is carefully
studied and analyzed. Central peak phenomena are ob-
served and discussed for both stress modulated and un-
stressed samples.

II. EXPERIMENTAL

The light scattering apparatus for simultaneous mea-
surement of Brillouin and Rayleigh scattering, including
the data acquisition system, has already been de-
scribed.[38-40] For this experiment a five-pass Fabry–
Perot interferometer configuration is employed in ad-
dition to the previously used three-pass configuration.
For 90° scattering experiments the three-pass inter-
ferometer configuration gives sufficient contrast and
signal to noise ratio from room temperature to 50 K
without any index matching liquid. However, for 180°
(back) scattering the three-pass configuration does not
give enough contrast, especially below 100 K and a five-
pass system must be employed. Two free spectral
ranges, 30 and 53 GHz, are used with effective finesse
of 40 to 45 maintained throughout the experiment dura-
tion. Brillouin spectra and correlation functions are
stored on a floppy disc on an HP9826 computer for
further calculations.

In addition to the experiments using a mechanical
refrigerator, a more conventional He cryostat, with a
temperature variation He chamber based on flowing gas
and liquid level position, was also employed in these
experiments. This new cryostat allows Rayleigh and
Brillouin spectra to be obtained under conditions free
from applied external periodic stress and thus intrinsic
central peak phenomena can be investigated.

The sample is mounted on a header which consists of
three main parts: a stainless steel tube from the top
flange to the sample compartment which provides sup-
port for the header, vacuum, gas inlet, and also car-
ries electrical lines between the sample and the top
flange; a copper isothermal can with three windows;
and a copper scattering cell wrapped with heater wire.
Samples are affixed to a copper block with GE 7031
varnish and placed in the copper scattering cell. This
is suspended within the isothermal copper can with three
thin stainless steel supports. This method of sample
support and isolation maintains an excellent thermal
stability and control at the samples. A small amount of
He gas is introduced into the isothermal can in order to
facilitate heat exchange. The entire lower portion of
the heater is immersed in liquid N_2 for the chloranil ex-
periments.

The temperature of the scattering cell is controlled by
a proportional controller; with a diode sensor as the
indicator, the cell temperature is regulated to within
± 0.1 K. Sample temperature is measured with a cop-
per constantan thermocouple placed just below the sam-
ple. Temperature fluctuations and drift are less than
1 μV for well over 24 h.

Single crystals of chloranil can be grown from satu-
rated solutions of benzene, toluene, chloroform, and
acetone by slow evaporation at room temperature.
Thick crystals are best grown from benzene and toluene
solutions. Single crystals up to $3 \times 4 \times 4$ to $5 \times 8 \times 8$ mm^3
can be readily grown. Each of them has a well defined
growth pattern such that the crystal could be aligned
visually. Two types of crystal shapes are employed in
this work: crystals with well developed hexagonal sur-
faces and crystals with well developed rhombic sur-
faces. For crystal axis assignment the angles between
surfaces were measured and the orientation determined
based on the assignment given in Ref. 11 for the type (a)
crystal.

The crystal is orange–yellow in color and transparent.
Since chloranil has very low solubility in most solvents,
is too soft to cut and polish, and is readily cleaved in
the (001*) plane, as grown surfaces are mainly em-
ployed for 90° scattering experiments. For back scat-
tering experiments, two kinds of samples are prepared
by cutting the crystal with a razor blade: crystals which
have a face perpendicular to the a or b axes. After a
large number of attempts, it is possible to prepare
crystals with good surfaces which give reasonable
Brillouin data for 180° scattering in a five-pass con-
figuration.

As the crystal absorbs blue light and local heating ef-
fects are even reported for 5145 Å, the laser power is
restricted to $\leq$ 50 mW at the sample. Even with this
low power, however, the obtained transition tempera-
tures are distributed over 90 to 92 K. This distribution
is clearly outside our temperature control and measure-
ment accuracy and suggests some degree of local heating
due to absorbed laser energy.

Several crystals have been annealed at 50 °C for about
50 h and examined by correlation spectroscopy and
Brillouin scattering. Identical Brillouin results obtain
from annealed and as grown samples of chloranil single
crystals.

III. RESULTS

Figure 1 presents the temperature dependence of pho-
nons propagating as depicted for the scattering geome-
try in Fig. 2(b). The c* axis is chosen to be perpen-
dicular to the ab plane which is always the largest sur-
face of the crystal. The scattering geometries actually
employed for 90° scattering experiments are shown in
Fig. 2; phonon propagation directions are also given.
Temperature dependences of the Brillouin shifts ob-
tained for such geometries are given in Fig. 3. In this
figure, phonons propagating along [101*] are denoted
by full circles. The QLA (quasilongitudinal acoustic)
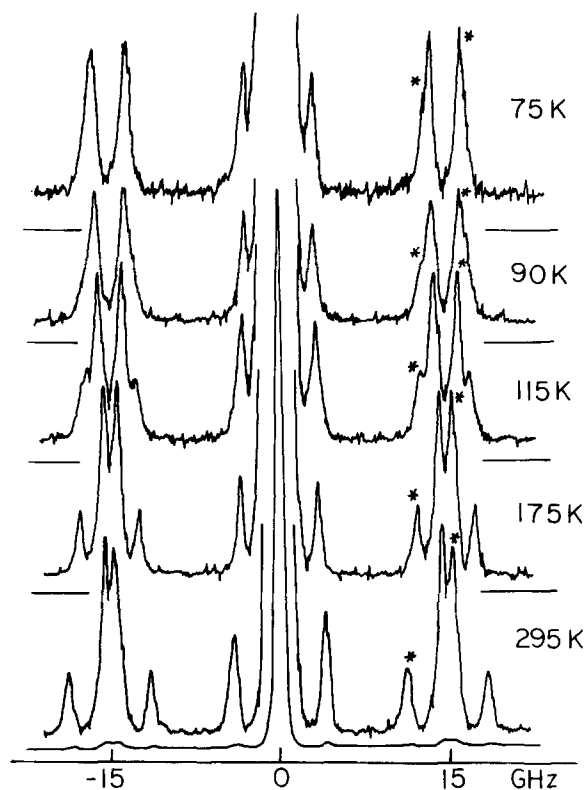mode at ~ 20 GHz exhibits a step function anomaly of

FIG. 1. Temperature development of the 90° scattering Brillouin spectrum of chloranil obtained by a three-pass interferometer. The scattering geometry for these data is shown in Fig. 2b. As the free spectral range is 30 GHz, features from different orders are overlapped. The phonon peaks in the overlap region which belong to the centered Rayleigh peak are denoted by * in the figure.
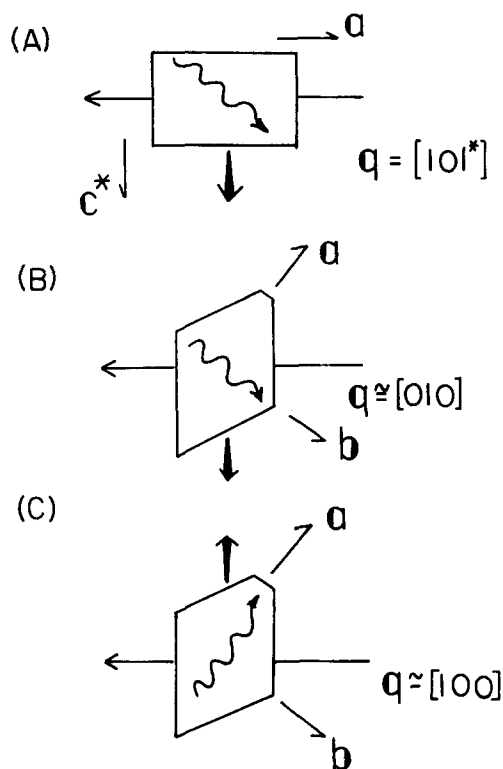

FIG. 2. The various scattering geometries employed to measure the 90° scattering spectra. The symbols are: wavy line: phonon progagation directions; thick arrow: scattered light observation direction; and thin arrow: incident laser light direction. The c* direction is defined to be a perpendicular direction to the ab plane which is always the largest surface of the crystal. The last index in the q direction is always with respect to c*. For geometries (B) and (C), propagation direction is only approximate due to crystal shape.

about 3% at the transition temperature. The other QTA phonons for this direction show monotonic increases in frequency as temperature decreases. At the transition temperature, the plots of Brillouin shift of these latter modes vs temperature evidence changes in their slopes.

The phonons observed in scattering geometry shown in Fig. 2(b) (denoted by open circles in Fig. 3) behave quite differently. The QLA-phonon mode exhibits a step function anomaly of about 1% (not shown in Fig. 3) at the transition temperature. The lowest frequency phonon in this set has a unique behavior. This frequency decreases as temperature decreases from room temperature to the transition temperature and becomes temperature independent in the low temperature phase to ± 2% (the experimental uncertainty). This mode has been extensively studied for several as grown as well as annealed crystals, as presented in Fig. 4. The temperature coefficient of this mode in the high temperature phase is

$$\delta(\Delta\nu_B)/\delta T \approx -4.5\times10^{-3} \text{ GHz/K} .$$

In order to obtain well-defined phonon frequency behavior around the transition temperature, back scattering experimental geometry has been employed for phonons propagating (nearly) along the [100*], [010*], and [001*] directions. Examples of back scattering spectra at room temperature are shown in Fig. 5. For the
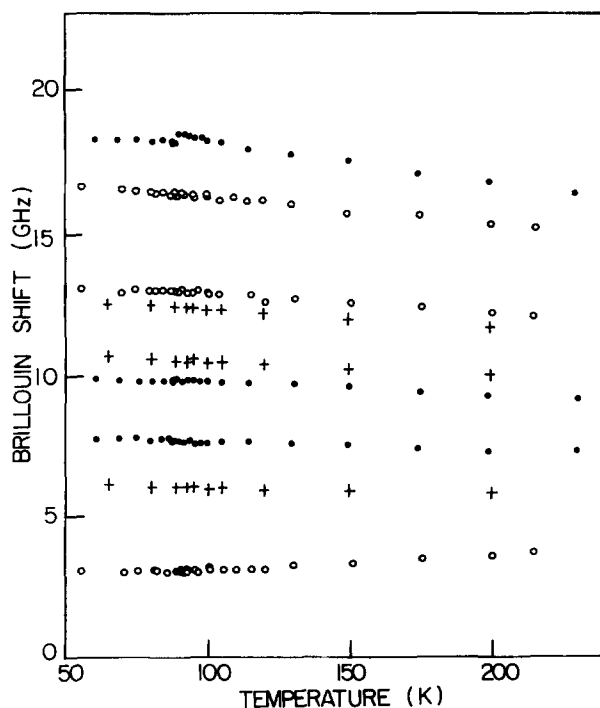

FIG. 3. Temperature dependence of the phonon frequencies obtained in the scattering geometries shown in Fig. 2. (●): Fig. 2a, (o): Fig. 2b, (+): Fig. 2c.
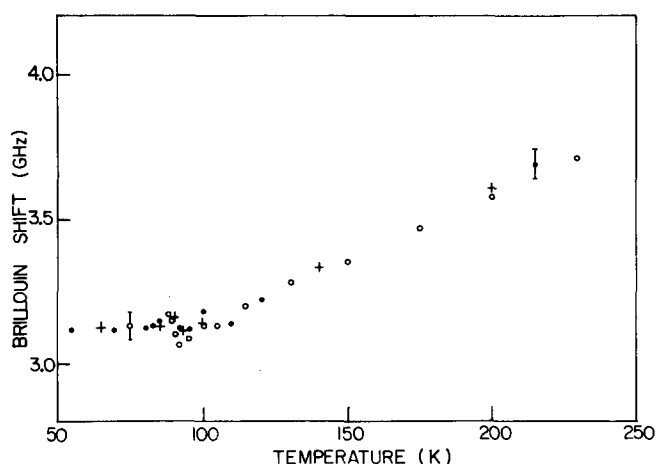
FIG. 4. Temperature dependence of the lowest frequency QTA phonon observed in the scattering geometry shown in Fig. 2b. (o): as grown sample A, (●): as grown sample B, (+): annealed sample C (50 °C for 50 h). From these results, the temperature coefficients can be defined as: $\delta(\Delta\nu_B)/\delta T \simeq -4.5 \times 10^{-3}$ GHz K for $T \geq T_c$ and $\delta(\Delta\nu_B)/\delta T \approx 0$ for $T \leq T_c$.

FIG. 6. Temperature dependence of the phonon frequencies (solid circles) and half-width (empty circles) in the [010*] direction obtained in back scattering. The transition temperature T_c has been determined from the anomaly observed around 16 GHz. The highest frequency phonon clearly exhibits a transition region below the actual transition temperature. The half-width evidences a peak centered around $T_c - 1$ K. Note that the frequency dependence in this transition is not monotonic; the frequency goes through a minimum prior to achieving its low temperature phase value at ~ 89 K.
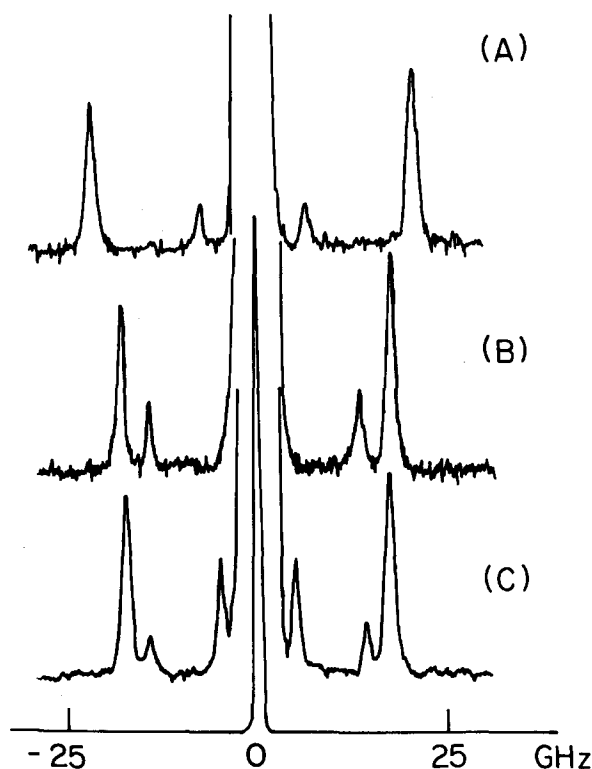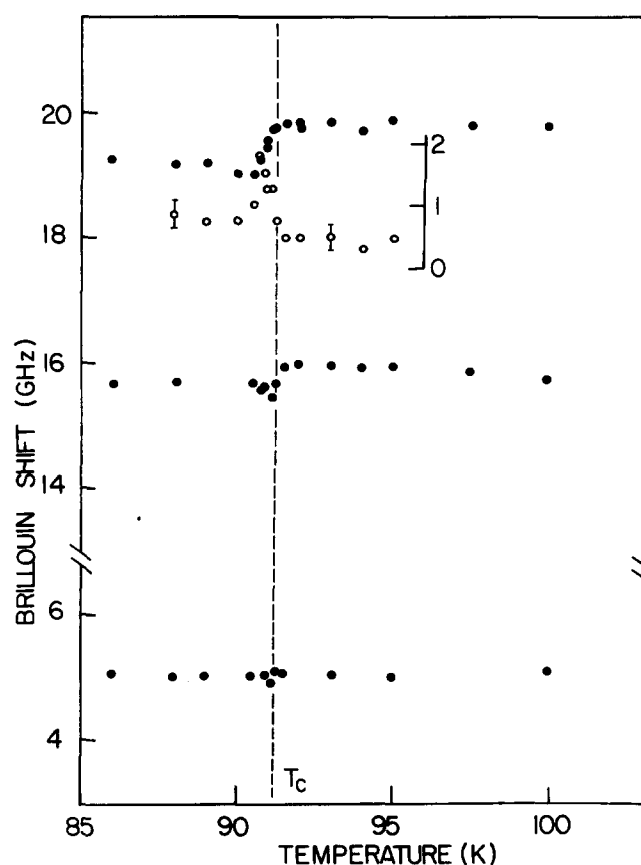

FIG. 5. Examples of back scattering Brillouin spectra obtained with five-pass interferometer configuration at room temperature with a 53 GHz free spectral range. (A): q ≈ [001 ≈ [001*], (B): q ≈ [100*], (C): q ≈ [010*]. In order to prevent pick-up of directly reflected laser light from the crystal surface, samples were tilted slightly in each scattering plane. Therefore, the phonons depicted propagate along directions ~ 5° from the well defined [100*], [010*], and [001*] directions. This geometry, then violates what would be Brillouin selection rules for the axis directions. Thus, for example, [010*] (C) spectra should only contain the LA phonon. No other problems arise from these small off-axis propagation directions.

[001*] and [100*] directions, only two phonon peaks could be observed. These phonon frequencies do not evidence any anomalous behavior within the experimental error. The temperature dependences of the b axis phonons, as observed in back scattering geometry, around the transition temperature are shown in Fig. 6. The lowest frequency mode possesses the negative temperature coefficient discussed above. At this wave vector, its temperature coefficient is $\delta(\Delta\nu_B)/\delta T \simeq -2.0 \times 10^{-3}$ GHz/K. The other phonons clearly exhibit anomalies around the transition temperature. The LA phonon possesses a step function anomaly with a transition region of about 1 K. The magnitude of the anomaly $[\delta(\Delta\nu_B)/\Delta\nu_B(95\ \text{K}) \sim 6\%]$ is close to the value obtained for the same mode in Ref. 15. The half-width at half-maximum of this LA phonon mode also exhibits anomalous behavior (broadening) around the transition temperature. As determined by the behavior of the other modes, the peak in the line width data of this mode appears below the transition temperature by about 1 K. Note also that the Brillouin frequency passes through a minimum value in the 1 K transition region
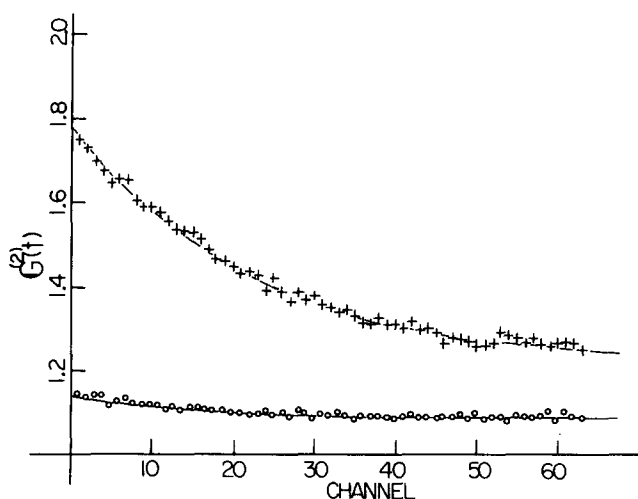
FIG. 7. Examples of external stress pulse induced intensity autocorrelation functions obtained under the following conditions: scattering geometry Fig. 2b; stress pulse direction: [001*]; sampling time: 0.1 ms; experiment duration: 500 s; correlation mode: full correlation; polarization: polarized. The (+) stands for as grown (unannealed) samples at 91.5 K and the (o) stands for annealed samples at 90 K. A simple exponential form was assumed for the correlation function $G^{(2)}(t)$ = $1 + \delta + A\, e^{-2t/\tau}$, in which δ, A, τ are fitting parameters. The numerical parameters are given in the text; the full lines represent least-squares fits of the above form. The annealed crystals correlation function is most likely due to incomplete annealing at the low temperature employed.

below T_c. This behavior is very similar to the previously reported QLA mode behavior in the a^* direction.[15]

Just as in benzil and urea,[38-40] an intensity autocorrelation function can be observed in as grown samples of chloranil. The correlation function appears only if an external periodic stress pulse, due to the helium refrigerator, is applied to the sample. In addition, a well-defined correlation function is also dependent on the direction dependence of the observed scattered light, the direction dependence of the applied stress pulse, and the polarization of the scattered light. In Fig. 7 an example of the observed correlation function at 91.5 K is shown by the daggers. The full line through the daggers is obtained by a least-squares fitting routine to a simple exponential form plus a variable base and is given by

$$G^{(2)}(t) = 1.21 + 0.578 \exp[-(2t/4.36 \text{ ms})] \, .$$

The scattering geometry shown in Fig. 2(b) with the stress pulse applied to the (001*) face gives a well-defined correlation function in polarized scattered light but not in depolarized scattered light (Fig. 7 conditions). The scattering geometry given in Fig. 2(c) with pulse on the (001*) face did not give any well-defined correlation function in either polarizations.

Annealing drastically reduces the amplitude of the correlation function as indicated in the set of open circles in Fig. 7. This data set is expressed as

$$G^{(2)}(t) = 1.08 + 0.047 \exp[-(2t/3.65 \text{ ms})]$$

and the curve for this equation is superimposed on the open circles. These results, of course, indicate that the correlation function, as in the case of urea and benzil, is associated with the forced motion of defects in the sample. In fact, the residual correlation found in "annealed" crystals is most likely due to inadequate annealing at too low a temperature.

The temperature dependences of the relaxation time and photon counting rate obtained in the scattering geometry shown in Fig. 2(b) with the same stress pulse on the (001*) face are shown in Fig. 8. Two experiments with the same sample are shown. As the temperature approaches the transition temperature in the high temperature phase, the relaxation times exhibit critical slowing down and the intensity rapidly increases. Although intensity and relaxation time show reproducible behavior in the high temperature phase, both exhibit extremely poor run-to-run reproducibility in the low temperature phase. Nonetheless, these two measureables I and τ, parallel one another for a given run.

The identical experiment has been carried out for annealed samples under the same conditions. At best only poor correlation functions could be observed as shown in Fig. 7 and, in addition, no anomaly in the relaxation times could be detected. The intensity of scattered
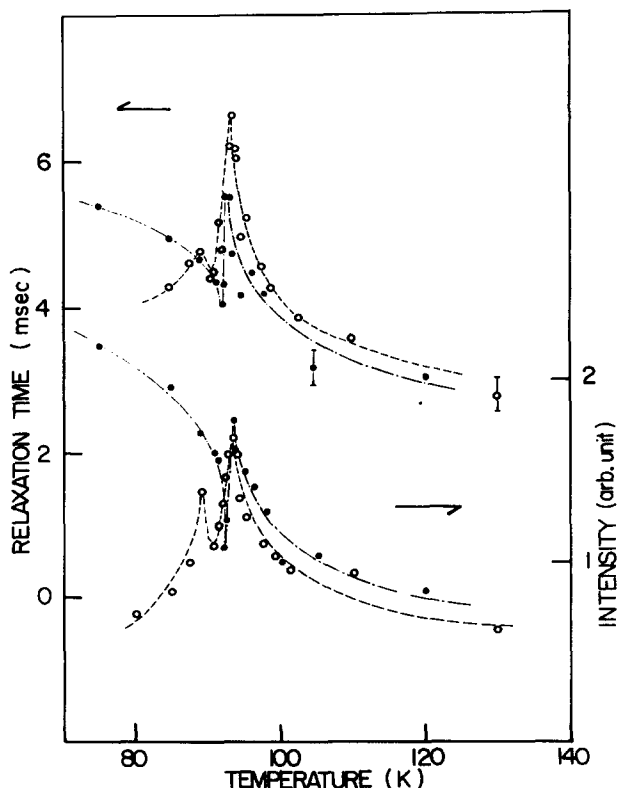

FIG. 8. Temperature dependences of relaxation times and intensities in a single sample. Experimental conditions are the same as given in Fig. 7. (o): run 1, (●): run 2. The lines are only to serve as guides for the eye. Note that the relaxation times and intensity parallel each other for a given run even in the low temperature phase. Below T_c the scattering intensity and relaxation time data are not consistent between runs.
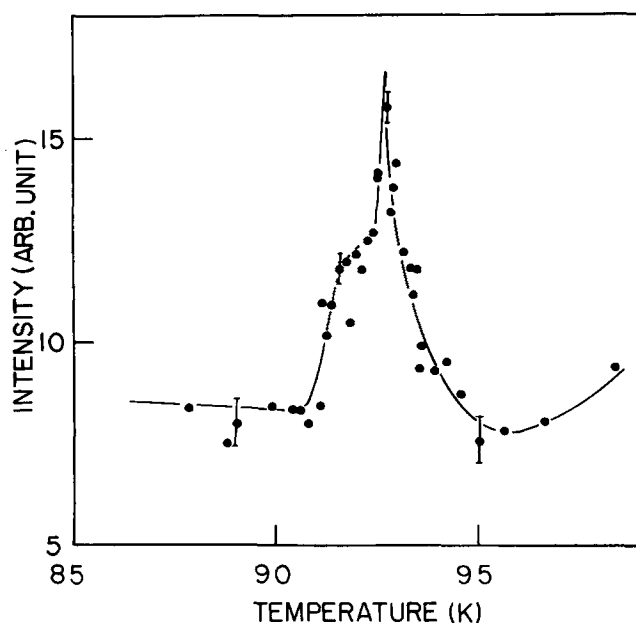
FIG. 9. An example of temperature dependence of the Rayleigh peak intensity obtained from the "unstressed" sample. Scattering geometry is shown in Fig. 2b. This set of data is obtained by using the Fabry–Perot interferometer. The correlator also gives similar behavior.

light, however, clearly exhibits an anomalous increase as temperature approaches the transition temperature in the high temperature phase. Cooling and heating runs give similar behavior on the high temperature phase; reproducibility in the low temperature phase, however, is once again quite poor. For the scattering geometry shown in Fig. 2(c), the observed correlation function is poorly defined and the relaxation time and intensity show only monotonic behavior through the transition region even for as grown crystals. The residual weak correlation function observed in annealed samples is considered to be due to poor annealing conditions at low temperature. At higher temperatures the crystals are vaporized and their surfaces made unsuitable for light scattering studies.

The Rayleigh component: QLA-phonon intensity ratio exhibits a similar increase in the high temperature phase as the temperature approaches T_c for the Fig. 2(b) geometry but not Fig. 2(c) geometry. The high temperature behavior is readily reproducible while the low temperature intensity ratio is not.

In addition to the "applied stress" light scattering results just mentioned, parallel studies have been carried out with samples not subjected to the cryorefrigerator stress pulse. Under these conditions, only intensity anomalies, not correlation functions, can be observed. The observed anomaly in the Fig. 2(b) geometry consists of at least two components: a sharp peak centered at the transition temperature and a shoulder in the low temperature phase. The sharp peak begins to appear around ($\sim T_c + 2$ K) or 95 K, possesses a maximum at the transition temperature, and exhibits a clear cut off in the low temperature phase. These data are shown in Fig. 9. The shoulder seems to be centered, from

run-to-run and sample-to-sample, around $T_c - 1$ K.

Several runs have been repeated for a number of as grown samples and the scattering light analyzed by both the autocorrelator and Fabry–Perot interferometer between 100 and 80 K. Although the above mentioned shoulder is always reproducible, its magnitude does vary from run-to-run and sample-to-sample. Through the phase transition, both techniques failed to detect any relaxation mode. The autocorrelator effectively covers the frequency range from 10 Hz to 1 MHz and the Brillouin apparatus has an instrumental width of 700 MHz under the conditions of the experiment. Therefore, the frequency width of the unresolved relaxation modes which cause the intensity anomalies must be outside these two ranges.

The scattering geometry depicted in Fig. 2(b) thus always exhibits an intensity anomaly independent of the experimental conditions: stressed, unstressed, annealed, unannealed. However, the scattering geometry depicted in Fig. 2(c) never evidences a central peak anomaly of any sort.

IV. DISCUSSION

These light scattering studies on the phase transition in chloranil have revealed several interesting and new results on the dynamics and statics of this system. The discussion below will concentrate on two areas in particular: (a) the elastic anomaly observed for the LA phonon mode ($\sim$ 20 GHz) propagating along $[010^*]$ and the Rayleigh central peak; and (b) the negative temperature coefficient obtained for the QTA phonon mode ($\sim$ 5 GHz) propagating in the same direction.

A. Elastic anomaly and Rayleigh central peak

As pointed out previously, the phase transition in chloranil at $\sim$ 93 K is induced by a Brillouin zone boundary instability at the $(0\,0\frac{1}{2})$ point. The order parameter for this transition can be taken to be a linear combination of molecular rotations around the axis perpendicular to the molecular plane and around the axis collinear with the C=O bonds. At this zone boundary point, the star of the wave vector has only one arm and the space group consists of four one dimensional small irreducible representations.[36] Therefore, the order parameter has only one component, η. For this second order transition the Landau free energy takes the form

$$F_\eta = \tfrac{1}{2} A\eta^2 + \tfrac{1}{4} B\eta^4 + \tfrac{1}{8} D\eta^6 + \cdots \ , \tag{1}$$

in which $A = \alpha(T - T_c)$. Including the elastic terms and interactions between strains and the order parameter, the full expression for the free energy is given by

$$F = F_\eta + F_{el} + F_{int} \ , \tag{2}$$

in which

$$F_{el} = \frac{1}{2} \sum_{i=1}^{6} c_{ii}^0\, e_i^2 + c_{12}^0 e_1 e_2 + c_{13}^0 e_1 e_3 + c_{23}^0 e_2 e_3$$
$$+ c_{15}^0 e_1 e_5 + c_{25}^0 e_2 e_5 + c_{35}^0 e_3 e_5 + c_{46}^0 e_4 e_6$$

and

$$F_{int} = -\tfrac{1}{2} (Ke_1 + Je_2 + Le_3 + Me_5 + Ne_4^2 + Pe_6^2)\, \eta^2 + \cdots \ .$$

For simplicity of discussion, off-diagonal terms such as $c_{ij}^0 e_i e_j$ will be neglected.[13] As there is no interaction between the strains under this assumption, the full free energy can be written as

$$F = \tfrac{1}{2} A \eta^2 + \tfrac{1}{4} B \eta^4 + \tfrac{1}{6} D \eta^6$$
$$+ \tfrac{1}{2} c_a^0 e_a^2 + \tfrac{1}{2} c_b^0 e_b^2 - \tfrac{1}{2} K e_a \eta^2 - \tfrac{1}{2} N e_b^2 \eta^2 + \cdots \qquad (3)$$

in which the bare elastic constant c_a^0 represents c_{11}^0, c_{22}^0, c_{33}^0, and c_{55} and c_b^0 represents c_{44}^0 and c_{66}^0. This simplified form still retains the essential features with respect to the phase transition of the full free energy given by Eq. (2).

If one ignores the contribution of the terms depending on e_b, the free energy, Eq. (3), has the same form as the one considered by Yao, Cummins, and Bruce[41] in their discussion of the acoustic anomalies in terbium molybdate near the improper ferroelastic–ferroelectric phase transition. The LA phonon propagating along [010*], which is specified by elastic constant c_{22}, couples to the order parameter η through the $e_a \eta^2$ interaction. Hence the techniques developed by Yao et al. are applicable here. Base on Ref. 41 the effective elastic constant c_a and the acoustic mode damping γ_a can be calculated from the elastic susceptibility which is given by the relation

$$\frac{1}{\chi_\epsilon(q, \omega)} = \frac{1}{\chi_\epsilon^0(\vec{q}, \omega)} - K^2 \eta_0^2 \chi_\eta^0(q - Q_B, \omega)$$
$$- \frac{1}{2} \frac{K^2 k_B T}{(2\pi)^4} \int d^3 Q \int \frac{d\Omega}{\Omega} \chi_\eta^{0\prime\prime}(Q, \Omega) \chi_\eta^0(\vec{q} - \vec{Q}, \omega - \Omega) . \qquad (4)$$

In this expression $\chi_\epsilon^0(q, \omega)$ and $\chi_\eta^0(Q, \Omega)$ are the zeroth-order susceptibilities for the strain and the mode which goes soft at $q = Q_B$ the $(0\,0\tfrac{1}{2})$ point, respectively, in the absence of coupling. The coupling parameter K is defined in Eq. (3) and η_0 is the order parameter. Q_B is the wave vector corresponding to the $(0\,0\tfrac{1}{2})$ point of the Brillouin zone. The zero-order strain susceptibility is

$$\chi_\epsilon^0(q, \omega) = \frac{q^2}{\rho} \Big/ [\omega_a^0(q)^2 - \omega^2 - i\gamma_a^0 \omega] , \qquad (5)$$

in which ρ is the density, the bare acoustic phonon frequency is given by

$$\rho [\omega_a^0(q)]^2 = c_a^0 q^2 ,$$

and γ_a^0 is the zeroth order phonon damping constant or linewidth. Neutron scattering measurements indicate that the zeroth order susceptibility χ_η^0 actually consists of contributions from a well-defined propagating soft mode plus a sharp central peak.[19] This three-peaked structure can be approximately represented by a susceptibility of the form[42]

$$\chi_\eta^0(Q, \Omega) = \chi_c^0(Q, \Omega) + \chi_s^0(Q, \Omega) \qquad (6)$$

with the soft mode part

$$\chi_s^0(Q, \Omega) = \frac{1}{m^*} \Big/ [\Omega_\eta(Q)^2 - \Omega^2 - i\Gamma(Q)\Omega] \qquad (7)$$

and the central component

$$\chi_c^0(Q, \Omega) = \frac{\delta(Q)^2}{\Omega_\eta(Q)^2} \Big/ [1 - i\Omega\tau(Q)] , \qquad (8)$$

in which

$$\tau(Q) = [\Gamma(Q) + \Omega_\eta(Q)^2 \tau_0(Q)]/\Omega_s(Q)^2 . \qquad (9)$$

The (renormalized) soft mode frequency is given by

$$\Omega_s(Q)^2 = \Omega_\eta(Q)^2 - \delta(Q)^2 . \qquad (10)$$

The phase transition takes place at a temperature T_c defined by $\Omega_s(Q_B) = 0$. $\delta(Q)$ and $\tau_0(Q)$ are parameters of the central peak component of χ_η^0 and $\Gamma(Q)$ is the damping constant for the propagating soft mode.

For the Brillouin component of $\chi_\epsilon(q, \omega)$, one may neglect the contribution to the susceptibility (Eq. (6)) from the central component, χ_c^0. In the limit of small acoustic phonon wave vectors q, the Ω-dependent integral in Eq. (4) can be evaluated to give[41]

$$\chi_\epsilon(q, \omega) = \frac{q^2}{\rho} \Bigg[\{\omega_a^0(q)^2 - \omega^2 - i\gamma_a^0 \omega\} - \frac{K^2 \eta_0^2 \, \omega_a^0(q)^2}{m^* c_a^0} \frac{\Omega_\eta^2(q - Q_B) - \omega^2 + i\Gamma(q - Q_B)\omega}{[\Omega_\eta(q - Q_B)^2 - \omega^2]^2 + \Gamma(q - Q_B)^2 \omega^2}$$

$$- \frac{1}{2} \frac{K^2 k_B T \, \omega_a^0(q)^2}{(2\pi)^3 m^{*2} c_a^0} \int d^3 Q \, \frac{1 - i \dfrac{\omega}{2\Gamma(Q)}}{1 - i \dfrac{\omega}{\Gamma(Q)}} \Big/ \{\Omega_\eta(Q)^2 [4\Omega_\eta(Q)^2 - \omega^2 - 2i\Gamma(Q)\omega]\} \Bigg]^{-1} . \qquad (11)$$

Taking the limits $\omega \ll \Gamma$ and $\omega \ll \Omega_\eta$, that is, excluding the immediate vicinity of the phase transition, one finds[41] for the effective elastic constant

$$c_a/c_a^0 = 1 - [K^2 \eta_0^2/(m^* c_a^0)] \Omega_\eta^2/(\Omega_\eta^4 + \Gamma^2 \omega^2)$$
$$- \tfrac{1}{2} (K^2 k_B T/[(2\pi)^3 m^{*2} c_a^0]) \int dQ/(4\Omega_\eta^4 + \Gamma^2 \omega^2) , \qquad (12)$$

and the acoustic phonon damping constant

$$\gamma_a = \gamma_a^0 + [K^2 \eta_0^2/(m^* c_a^0)] \Gamma/(\Omega_\eta^4 + \Gamma^2 \omega^2)$$
$$+ \tfrac{1}{2} (K^2 k_B T/[(2\pi)^3 m^{*2} c_a^0]) \int \Gamma \, dQ/[2\Omega_\eta^2(4\Omega_\eta^4 + \Gamma^2 \omega^2)] . \qquad (13)$$

In the second terms of Eqs. (12) and (13), $\Omega_\eta = \Omega_\eta(q - Q_B)$ and $\Gamma = \Gamma(q - Q_B)$ but in the last terms of these equations $\Omega_\eta = \Omega_\eta(Q)$ and $\Gamma = \Gamma(Q)$. If one neglects fluctuation contributions, represented by the last terms in Eq. (12) and (13), these expressions are identical to the ones proposed by Hauret and Benoit and others to describe Debye type relaxation in other systems.[35,43,44]

An examination of Eqs. (4), (11), (12), and (13) indicates that there are two corrections to the bare elastic constant c_a^0 and the bare damping constant γ_a^0. The first represents a mean field Landau–Kalatnikov type contribution[45] associated with the coupling $-K\eta_0 e_a \eta$, in which η_0 is the equilibrium value of the order parame-

ter, assumed to have the form

$$\eta_0 = \begin{cases} 0, & T > T_c , \\ \eta_0^0 (T_c - T)^\beta , & \beta = 0.33, \ T < T_c . \end{cases}$$

In Eq. (14) T_c is the transition temperature as defined by Eq. (10). For the Q dependence of the soft mode frequency $\Omega_\eta(Q)$, which appears in Eqs. (8)–(13), we follow the arguments of Yao et al.[41] and assume the approximate dispersion relation:

$$\Omega_\eta(Q_B + Q_x \, a^*/a^* + Q_y \, b^*/b^* + Q_z \, c^*/c^*)^2$$

$$= \Omega_\eta(Q_B)^2 + a_\eta^2(Q_x/a^*)^2 + b_\eta^2(Q_y/b^*)^2 + c_\eta^2(Q_z/c^*)^2 , \qquad (15)$$

in which a^*, b^*, and c^* are the reciprocal lattice vectors. Note that a^* and c^* are not perpendicular. The parameter c_η is specified by the relation

$$c_\eta^2 = \Omega_\eta(0)^2 - \Omega_\eta(Q_B)^2 , \qquad (16)$$

with similar expressions holding for a_η and b_η. From neutron scattering results[19] we estimate the ratios of $\Omega_\eta(Q_a) : \Omega_\eta(Q_b) : \Omega_\eta(0)$ as $1.5 : 4 : 1$, with Q_a and Q_b representing the zone boundary in the a^* and b^* directions when Q_B is taken as the center of the Brillouin zone. The temperature dependence of the zone boundary soft mode has the form[14,19]

$$\Omega_\eta(Q_A) = \begin{cases} k(T - T_0)^{1/2\gamma} , & T > T_c , \\ k'(T_0' - T)^{1/2\gamma'} , & T < T_c . \end{cases} \qquad (17)$$

with $k' = \sqrt{2}k = 1.48$ cm^{-1}/K$^{1/2}$ and $\gamma = \gamma' = 1$.[14] If the parameter δ, defined in Eqs. (8) and (10), is nonzero, the temperatures T_0 and T_0' will be different from T_c.

For c_a in the low frequency limit the Landau–Kalatnikov contribution to $\Delta c_a = c_a - c_a^0$ is proportional to $(\eta_0/\Omega_\eta)^2$ $\propto (T_c - T)^{2\beta - \gamma'}$ for $T < T_c$ if T_0' in Eq. (17) is the same as T_c, that is, very small δ. In that case one also finds $\Delta\gamma_a = \gamma_a - \gamma_a^0 \propto \eta_0^2 \Gamma/\Omega_\eta^4 \propto (T_c - T)^{2\beta - 2\gamma'}$. In the high temperature phase these terms do not contribute to either c_a or γ_a. Landau theory predicts $2\beta = \gamma' = 1$ and therefore a step function decrease in c_a and a positive contribution to $\Delta\gamma_a \propto (T_c - T)^{-1}$ for $T < T_c$. However, neutron inelastic scattering experiments[19] and Raman measurements[13,14] give $\beta \cong 0.33$ and $\gamma' \cong 1$ so that $2\beta - \gamma' \cong -0.34$ and $2\beta - 2\gamma' \cong -1.34$. These Landau–Kalatnikov terms contribute only below T_c and can not explain the entire anomaly.

The second term which contributes to Eqs. (12) and (13), above the transition as well as below it, comes from the anharmonic coupling to critical fluctuations[41] and is represented by the last term in Eq. (4). It leads to a rounding off of the discontinuities in c_a and γ_a for $T > T_c$ and generates an additional contribution in the low temperature phase. The integrals over the wave vectors Q of the Brillouin zone in Eqs. (4), (11), (12) or (13) are performed in the manner outlined in Ref. 41, centered at the point $(0, 0, \frac{1}{2})$ or Q_B. Because of the Ω_η factors in the denominators, the integrals are heavily weighted towards points close to $(0, 0, \frac{1}{2})$. Hence the exact shape of the Brillouin zone boundary is not expected to be a major factor in the value of the integral. In the present case, the zone was taken as a distorted
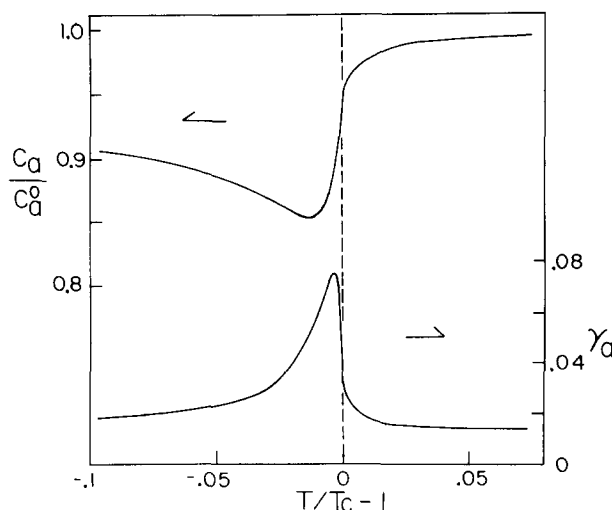

FIG. 10. Predicted temperature dependence of the reduced elastic constant c_a/c_a^0 and the linewidth γ_a.

sphere with the same volume as the actual Brillouin zone.

It should be noted that Eqs. (4)–(10) represent a simplified model for the phonon–phonon susceptibility. No attempt has been made to identify specific combinations of elastic constants pertinent to particular longitudinal or transverse acoustic modes.

The results for the reduced effective elastic constant c_a/c_a^0 and the damping constant γ_a, as calculated from Eqs. (4)–(10) are shown in Fig. 10. Numerical evaluation shows that the approximate relations (12) and (13) give almost the same results as the general approach (4). No serious attempt was made to provide a quantitative fit to the results shown in Fig. 6. The parameter values used for the plots of Fig. 10 are (ω, γ have units of cm^{-1})

$$\omega_a^0 = 0.667 , \quad \gamma_a^0 = 0.015 , \quad \Gamma = 2 , \quad \delta = 0.1 ,$$

$$\tau_0 = 200 , \quad \kappa_1 = K^2/(m^* \, c_a^0) = 5$$

and

$$\kappa_2 = \frac{1}{2} K^2/[(2\pi)^3 \, m^{*2} \, c_a^0 \, \nu_{BZ}] = 100 ,$$

with ν_{BZ} being the volume of the first Brillouin zone. It is found that the behavior of c_a and γ_a in the high temperature phase depends only on κ_2, whereas the low temperature behavior is sensitive mainly to κ_1. It should be pointed out that the present theory describes the behavior of the elastic constants of type c_a only. The acoustic phonon frequencies measured along the various symmetry directions generally depend on several elastic constants and hence may show slightly different behavior.

In these calculations we further assume a small, but finite, value of the acoustic phonon wave vector $|q|$ $\cong 10^{-3} Q_B$. The effect of finite q is to smooth out the discontinuity in c_a and the singularity in γ_a. Figure 10 clearly shows that maximal line width broadening occurs at a temperature T_M greater that T_m, the temperature of the minimum of c_a. We estimate $T_M - T_m$ to be of the order of 1 K. Both T_M and T_m fall below the transition

temperature T_c. Such behavior is qualitatively the same as that observed for K_2SeO_4 by Hauret and Benoit[43] who provided an explanation using Debye type relaxation. Since they included only Landau–Kalatnikov type terms they were of course not able to explain the behavior above T_c.

The contributions of the fluctuations to the elastic constant (12) and the linewidth (13) can be observed in the high temperature phase where they are not over-shadowed by mean-field type contributions. The critical behavior has been examined by Schwabl[42] for the ABO_3 perovskites in which a $\frac{1}{2} Ke_a \eta^2$ type coupling is also found. In this case the change in the longitudinal mode elastic constant is

$$\Delta c_l \propto - (T - T_c)^{-\alpha} ,$$

which is proportional to the negative of the specific heat. For a transverse mode the predicted behavior is[42]

$$\Delta c_t / c_t \propto - (T - T_c)^{-\nu_d (1 - 2\eta_d)} .$$

The power laws for sound attenuation predicted by Schwabl are

$$\alpha^l(\omega) \propto \omega^2 (T - T_c)^{-\rho} , \quad \alpha^t(\omega) \propto \omega^2 (T - T_c)^{-\rho'} .$$

Although it is reasonable to assume analogous behavior in chloranil, the present measurements are not detailed enough to examine the behavior near T_c.

Previous investigators have identified the molecular motions corresponding to the zone boundary soft mode as out of phase rotations about one or more molecular axes.[18,19] Hence, it might be reasonable to assume that m^* in Eqs. (7) and (11)–(13) represents an effective moment of inertia per unit volume. For chloranil the rotational constant for rotations about the axis perpendicular to the molecular plane is $B_Z = \hbar^2/(2I_2) \cong 10^{-2}$ cm^{-1} and the moment of inertia about an axis in the molecular plane is of the same order of magnitude. This means that since $\kappa_1 \propto 1/m^*$ and $\kappa_2 \propto 1/m^{*2}$ the value of κ_2 should be much smaller than κ_1. The opposite, that is $\kappa_2/\kappa_1 \cong 20$, must be assumed to obtain reasonable agreement with the experimental results for the high temperature phase.

The phonon–phonon correlation function is calculated from Eq. (4) and the relation for the scattering function is found to be

$$S(\mathbf{q}, \omega) = \frac{2}{1 - e^{-\beta\omega}} \chi_\epsilon''(\mathbf{q}, \omega) ,$$

in which χ_ϵ'' is the imaginary part of the elastic susceptibility. Because of the three-peaked nature of the zeroth order susceptibility χ_η^0, $S(\mathbf{q}, \omega)$ shows a central peak at $\omega = 0$ in addition to the Brillouin peaks at $\omega = \pm \omega_a$. Like the Brillouin response, the central peak consists of two parts: a Landau–Kalatnikov contribution which contains the factor η_0^2 and a contribution from the fluctuations. The Landau–Kalatnikov part of $S(\mathbf{q}, 0)$ has its maximum at a temperature slightly below T_c because of the competition between the temperature dependences of η_0^2 and Ω_η^2. However, the fluctuation contribution to $S(\mathbf{q}, 0)$ will peak at $T = T_c$. Hence, a multiple-peaked Rayleigh intensity such as observed in unannealed samples under conditions of no applied stress (Fig. 9) might
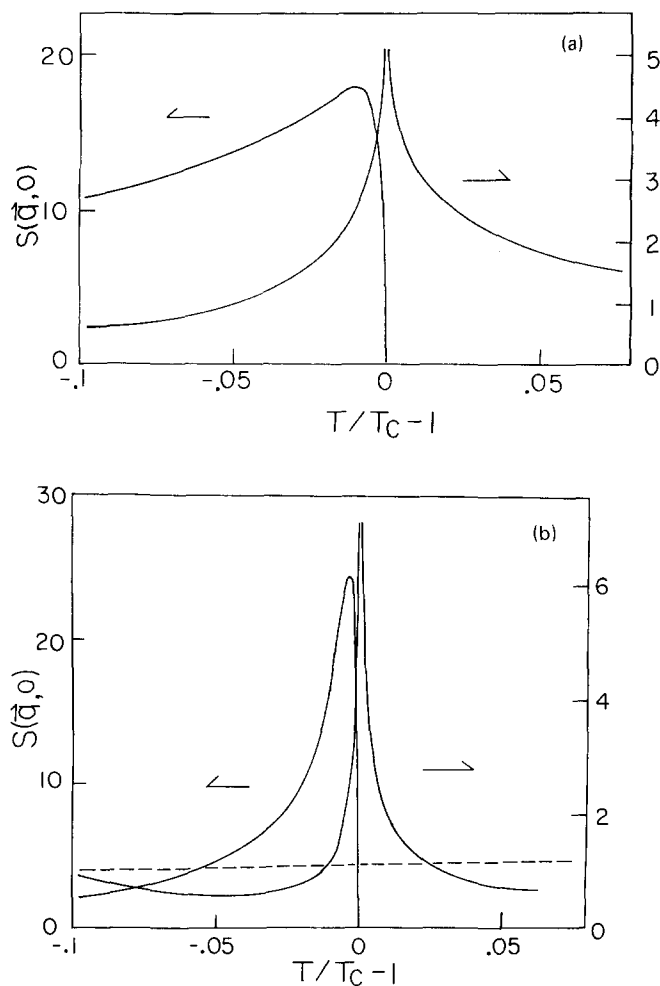

FIG. 11. Predicted frequency dependence of the phonon–phonon correlation function $S(\mathbf{q}, 0)$. The central peak contributions, arising from both mean field and flucturation terms, are shown in part (a). The corresponding soft mode contributions, as well as the contribution of the bare acoustic photon, are shown in part (b). This figure illustrates how the various contributions add to give a multiply peaked $S(q, 0)$. No attempt is made to fit the data of Figs. 7, 8, and 9.

be explained in this manner. However, a quantitative explanation of this temperature behavior of the Rayleigh intensity is probably more complex.

To explain the observed behavior of the Rayleigh scattering intensity (Fig. 9) we show the temperature dependences of the various contributions to $S(\mathbf{q}, 0)$ in Fig. 11. Part (a) shows the mean field and fluctuation contributions to $S(\mathbf{q}, 0)$ arising from the central peak part of χ_η^0, that is Eq. (8). Part (b) gives the mean field and fluctuation contributions arising from the soft mode contribution Eq. (7). We show only the qualitative behavior of each contribution; no attempt was made to adjust the vertical scales. The background contribution due to the "bare" acoustic phonon is shown separately in Fig. 11.

The relation between intensity and correlation time anomalies is treated in other publications from this laboratory.[38–40] We note here only that the defect modu-

lation and "intrinsic" light scattering both arise from
the basic underlying lattice dynamics.

B. Negative temperature coefficient for the QTA phonon

The lowest frequency QTA phonons propagating along
the direction given by Fig. 2(b) and the [010*] direction
possess negative temperature coefficients $\delta(\Delta\nu_B)/\delta T$
$\approx -4.5\times10^{-3}$ GHz/K and -2.0×10^{-3} GHz/K, respective-
ly, in the high temperature phase and are temperature
independent in the low temperature phase. The fre-
quency of the mode propagating along the [010*] direc-
tion, for simplicity, is governed by an elastic constant

$$\{(c_{44}+c_{66}) - [(c_{44} - c_{66})^2 + 4c_{46}^2]^{1/2}\}/2 \ . \tag{18}$$

This phonon, a combination of strains e_4 and e_6, inter-
acts with the order parameter by quadratic-quadratic
coupling as given in Eq. (2). As already pointed out,
Landau theory predicts that such interactions do not af-
fect the elastic behavior in the high temperature phase
but change the slope of the temperature phase.

Recent Raman scattering work reported a similar be-
havior for an optical phonon mode around 16 cm^{-1} (room
temperature).[14] This optical phonon mode possesses a
temperature coefficient of $\delta\nu/\delta T \approx -3\times10^{-3}$ cm^{-1}/K in
the high temperature phase and stiffens in the low tem-
perature phase. This behavior is quite similar to the
QTA~[010*] temperature dependence discussed above.
It is possible that this optical phonon is a soft mode
which can interact with the QTA modes resulting in the
observed Brillouin scattering behavior.

The purpose of this section of the discussion is to
present a plausible explanation for the behavior of the
QTA-phonon frequency in the high temperature phase.
Three possibilities will be considered: (1) anharmonic
interactions between the QTA phonon and the order pa-
rameter; (2) accidental behavior; and (3) a soft optical,
mode related to a phase transition not realized, which
is coupled to the transverse acoustic modes.

1. Anharmonic interactions

As mentioned above, the biquadratic coupling between
the order parameter and the elastic modes does not af-
fect the elastic properties within the Landau theory for
the high temperature phase. However, fluctuations of
the order parameter $\langle\eta^2\rangle$ can contribute to the elastic be-
havior even in the high temperature phase. To illustrate
this point, the interactions can be extended as follows:

$$Ne_b^2\eta^2 \to \sum_{\{k\}} N(k_1 k_2 k_3 k_4) e_b(k_1) e_b(k_2) \eta(k_3) \eta(k_4) \delta(\Sigma_i k_i)$$

$$\approx \sum_{k, k'} N(k - k k' - k') e_b(k) e_b(-k) \langle\eta(k')\eta(-k')\rangle$$

$$\propto \sum_k \left\{ \sum_{k'} N(k - k k' - k') \frac{k_B T}{\Omega_s(k')} \right\} e_b(k) e_b(-k) \tag{19}$$

with $\Omega_s(k)$ defined by Eq. (10) and the high temperature
approximation has been used. Therefore, the renor-
malized elastic constants c_b can be written

$$c_b(k) \approx c_b^0 + \sum_{k'} \frac{N(k - k k' - k')}{|k|^2} \frac{k_B T}{\Omega_s(k)}$$

$$= c_b^0 + \sum_{k'} \theta(k')T \ [T - T_c(k')]^{-1/2} \ , \tag{20}$$

in which

$$\theta(k') = \lim_{k\to 0} \frac{N(k - k k' - k')}{|k|^2} k_B \left\{ \frac{T - T_c(k')}{\Omega_s(k')^2} \right\}^{1/2} \ .$$

In the low temperature phase one obtains

$$c_b = c_b^{0'} + 2 \frac{N(k - k k_B - k_B)}{|k|^2} \langle\eta_{k_B}\rangle^2$$

$$+ \sum_{k'} \theta'(k') T(T_c(k') - T)^{-1/2} \ , \tag{21}$$

in which

$$\theta'(k') = \lim_{k\to 0} \frac{N(k - k k' - k')}{|k|^2} k_B \left\{ \frac{T_c(k') - T}{-2\Omega_s(k')^2} \right\}^{1/2} \ .$$

The first two terms on the right-hand side of Eq. (21)
are equivalent to the Landau theory result in Eq. (13),
and the last term gives the fluctuation contribution in
the low temperature phase.

As the elastic constant is almost temperature inde-
pendent in the low temperature phase, one might expect
a cancellation of the last two terms in Eq. (21); i.e.,

$$\frac{2N(k - k k_B - k_B)}{|k|^2} \langle\eta_{k_B}\rangle^2 + \sum_{k'} \theta'(k')T [T_c(k') - T]^{-1/2} \approx 0 \ . \tag{22}$$

There are two fundamental difficulties with this model.
First, the negative temperature behavior of the QTA
phonon can be observed around room temperature for
which the fluctuations would be expected to be small.
The slopes $\delta(\Delta\nu_B)/\delta T \sim -2\times10^{-3}$ and -4.5×10^{-3} GHz/K
are almost constant throught the high temperature
phase. If anharmonic interactions were responsible
for the negative temperature behavior, the slope might
well be a function of temperature, especially in the
vicinity of T_c. Second, the assumed cancellation [Eq.
(22)] seems doubtful as the first term increases (due to
the temperature dependence of the order parameter)
while the second term decreases as temperature de-
creases from the transition temperature. Thus, we
find this mechanism possible but less likely than the
others.

2. Accidental behavior

To see how this may occur, assume an inequality be-
tween the elastic constants appearing in Eq. (18), such
that,

$$c_{44} \gg c_{46} \gtrsim c_{66} \tag{23}$$

or equivalently

$$c_{66} \gg c_{46} \gtrsim c_{44} \ . \tag{23'}$$

Then the lowest phonon frequency for the direction under
consideration ([010*]) will be governed by

$$c_{66} - c_{46}^2/c_{44} \tag{24}$$

or

$$c_{44} - c_{46}^2/c_{66} \ . \tag{24'}$$

The elastic constants c_{44} and c_{66} can be directly measured by back scattering techniques in the [100*] and [001*] directions. As shown in Fig. 5, only two phonon peaks could be observed in these directions. Low crystal symmetry prevents the identification of this TA mode by polarization and selection rule studies. No anomalous behavior could be detected for these TA phonons by back scattering experiments. Combining the results shown in Fig. 3, the elastic constants c_{44} and c_{66} can be expected to behave normally. If the elastic constant c_{46} possesses a stronger temperature dependence in the high temperature phase then either c_{44} or c_{66}, the phonon frequency will exhibit the observed behavior in the high temperature phase. There is no particular reason, however, to believe such an accidental behavior and cancellation in the low temperature phase would have to occur.

The major problem or inadequacy with this model is that it leaves the question of the Raman observed optical mode temperature dependence to be discussed in a completely separate and independent manner.

3. Soft mode

This mechanism seems to be the most reasonable explanation as it presents a unified understanding of the QTA and Raman mode behavior taken together.

Assume that chloranil undergoes (or would undergo) a Brillouin zone center driven phase transition, the order parameter for which belongs to the B_g irreducible representation of the C_{2h} point group.[10] [It should be noted however, that a conflicting assignment also exists in the literature suggesting this 16 cm^{-1} feature may be of A_g symmetry. We have repeated these studies and our polarized Raman scattering results are in substantial agreement with those of Ref. 10 indicating a B_g assignment. Of course, the following discussion holds in the stated coupling order only if the B_g symmetry assignment is correct.] The transition must take place below 90 K and is thus never realized. These ideas can be formally expressed as

$$F = \tfrac{1}{2} A\eta^2 + \tfrac{1}{4} B\eta^4 + \tfrac{1}{6} D\eta^6 + \tfrac{1}{2} \omega_R^2 R^2 + \tfrac{1}{2} c_b^0 e_b^2$$
$$- \tfrac{1}{2} N e_b^2 \eta^2 - \tfrac{1}{2} V\eta^2 R^2 - WRe_b + \cdots , \quad (25)$$

in which ω_R is the Raman frequency and R is the Raman optical mode coordinate. For the Raman mode we assume a weak temperature dependence of the form

$$\omega_R^2 = \alpha_R(T - T_R) , \quad T > T_c . \quad (26)$$

This assumption is consistent with the Raman data for the 16 cm^{-1} phonon.[14] Although Raman frequencies usually increase with decreasing temperature due to crystal anharmonicity, this mode evidences the opposite behavior as T approaches T_c.[14] However, we expect $T_R \ll T_c$. With the assumption as stated in Eq. (26), the usual procedures in dealing with the Landau free energy Eq. (25) yield

$$c_b = c_b^0 \frac{T - T_R''}{T - T_R'} - N\eta_0^2 , \quad (27)$$

and

$$\omega_R^2 = \alpha_R(T - T_R) - V\eta_0^2 , \quad T < T_c , \quad (28)$$

in which

$$T_R' = T_R + V\eta_0^2 \quad (29)$$

and

$$T_R'' = T_R' + \frac{W^2}{c_b^0 \alpha_R} . \quad (30)$$

From the Raman data[14] it follows that T_R is large and negative and $V < 0$. From the Brillouin data, as shown in Fig. 4, $N < 0$. Hence for $T > T_c$ and $\eta_0 = 0$, we expect $T_R'' > T_R$ so that the temperature dependence of c_b is expected to be much more noticeable than that of ω_R. From Eqs. (27) and (28) it is expected that both ω_R and c_b show discontinuities in their slopes at the transition. These are indeed found in the Raman data[14] and in Fig. 4.

In this model, two independent soft modes or instabilities, one at the zone center and one at the zone boundary (for which $T_c = 93$ K) are introduced. For chloranil the two apparent instabilities are quite separated in temperature and the transition temperature for the zone center mode (T_R in the above) is probably large and negative. Such behavior can be compared with that of other well studied molecular crystals. A bilinear coupling between strains and very weakly temperature dependent Raman modes is found to provide a satisfactory explanation for the phase transition in s-triazine.[39] On the other hand, the situation is more complicated for the case of benzil, in which both bilinear and linear-quadratic couplings are thought to be important. The mechanism for the phase transition in benzil is thought to be a triggering of an M-point zone boundary instability by a Γ point one.[46-48] The differences between these apparently diverse phase transitions most likely lie in differences in the values of the coupling constants in Eqs. (3) and (25).

V. CONCLUSIONS

The nonferroic phase transition in chloranil at ~ 93 K has been examined by Brillouin scattering and correlation spectroscopy. Our findings can be summarized as follows:

(1) The LA phonon propagating along the [010*] direction exhibits a step function anomaly (~ 6%) at the transition temperature. There is a transition region for this frequency change, the width of which is about 1 K, just below the transition temperature T_c. The half width at half maximum for this phonon also has an anomalous broadening around the transition temperature. The Brillouin shift near the phase transition falls to a minimum value in this transition region.

(2) The lowest frequency QTA phonon propagating around the [010*] direction evidences a negative temperature coefficient in the high temperature phase $\delta(\Delta\nu_B)/\delta T \simeq -2 \times 10^{-3}$ GHz/K. This mode becomes temperature independent in the low temperature phase. This behavior can be observed for the other QTA phonon propagating around the [010*] direction.

(3) Other acoustic phonons simply undergo changes of slope $\delta(\Delta\nu_B)/\delta T$ at the transition temperature with the slopes all being positive in both phases.

(4) External stress induced relaxation processes can be observed by correlation spectroscopy. A well defined correlation can only be observed in polarized scattered light and for specific scattering and pulse direction geometries.

(5) Relaxation time and intensity of scattered light associated with the correlation function show anomalies around the transition temperature for as grown samples. Annealed samples in the same experimental geometries do not evidence the relaxation time anomaly but do show an intensity anomaly.

(6) Samples not subjected to stress modulation also show at least two central peak intensity anomalies around the transition temperature (one below T_c and one at T_c).

With the exception of the negative temperature coefficient for the low frequency QTA phonon propagating around the [010] direction, Brillouin scattering results can be interpreted by variations on and elaborations of Landau theory. The b-axis LA phonon with a large step function anomaly can be understood by a Landau–Khalatnikov process and anharmonic coupling to order parameter fluctuations.

In order to explain the negative temperature coefficient observed for the QTA phonon propagating around the [010] direction, three possibilities have been considered: anharmonic coupling between the strains and the order parameter, accidental cancellation and/or relations between certain elastic constants, and a temperature dependent Raman active mode related to a postulated but unrealized phase transition. The last possibility seems to give the most reasonable explanation, not only to the QTA-phonon behavior, but also to a Raman mode possessing similar high temperature phase behavior.

The Rayleigh intensity anomalies observed under unstressed conditions can be interpreted as intrinsic phenomena related to the zone boundary soft phonon-central peak response. An understanding of these anomalies near T_c arises naturally within the context of the Yao, Cummins, Bruce,[41] Landau type theory employed above to explain the LA-phonon behavior (c_{11}). The theory can qualitatively explain the observed multipeak nature of the anomalies encompassing both the central peak and soft phonon responses. Brillouin and Rayleigh techniques have not, however, detected any relaxation mode at the zone center. This suggests that the width of the relaxation mode which induces these intensity anomalies is either between 10 and 700 MHz or less than 10 Hz.

On the other hand, the relaxation processes observed under stress conditions clearly exhibits the stress-defect related characteristics previously reported for benzil[38] and urea.[40] Thus, the chloranil results can also be discussed in terms of the anelastic solids model developed for the benzil data by including the soft phonon-central peak response. The actual calculation in this instance becomes very complicated due to the scattering geometry employed and the lower crystal symmetry. The theory predicts a general relation between the anomalous parts of the relaxation time $(\Delta\tau)$ and intensity (ΔI) given

by

$$\Delta I \sim (\Delta\tau)^2 \ .$$

The chloranil data seem to support this general relation.

[1] S. C. Chu, G. A. Jeffrey, and T. Sakurai, Acta Crystallogr. 15, 661 (1962).
[2] C. B. Richardson, J. Chem. Phys. 59, 5392 (1973).
[3] H. Chihara and N. Nakamura, J. Chem. Phys. 59, 5392 (1973).
[4] H. Chihara and K. Masukane, J. Chem. Phys. 59, 5397 (1973).
[5] H. Terauchi, T. Sakai, and H. Chihara, J. Chem. Phys. 62, 3832 (1975).
[6] D. M. Hanson, J. Chem. Phys. 63, 5046 (1975).
[7] I. V. Ismestiev and G. B. Soifer, Phys. Status. Solidi B 54, K33 (1972).
[8] G. Jugie and J. A. S. Smith, J. Chem. Soc. Faraday Trans. 2 71, 608 (1975).
[9] H. Chihara and N. Nakamura, J. Phys. Soc. Jpn. 44, 1567 (1978).
[10] A. Girlando and C. Pecile, J. Chem. Soc. Faraday Trans. 2 69, 1291 (1973).
[11] H. Yamada, M. Saheki, S. Fukushima, and T. Nagasao, Spectrochim. Acta Part A 30, 295 (1974).
[12] A. Girlando, I. Zanon, R. Bozio, and C. Secile, J. Chem. Phys. 68, 22 (1978).
[13] M. Wada, H. Shichi, A. Sawada, and Y. Ishibashi, J. Phys. Soc. Jpn. 49, 1892 (1980).
[14] A. Girard, Y. Delugeard, C. Ecolivet, and H. Cailleau, J. Phys. C 15, 2127 (1982).
[15] C. Ecolivet, Solid State Commun. 40, 503 (1981).
[16] K. J. Weperen and G. J. Visser, Acta Crystallogr. Sect. B 28, 338 (1972).
[17] J. L. Baudour, Y. Delugeard, H. Cailleau, M. Sanquer, and C. M. E. Zeyen, Acta Crystallogr. Sect. B 37, 1553 (1981).
[18] J. L. Baudour and J. Meinnel, Acta Crystallogr. Sect. B 38, 472 (1977).
[19] (a) W. D. Ellenson and J. K. Kjems, J. Chem. Phys. 67, 3619 (1977); (b) J. L. Bandour, J. Meinnel, A. Girard, and Ch. Vettier, J. Phys. C 15, 5003 (1982).
[20] P. Toledano and J. C. Toledano, Phys. Rev. B 25, 1946 (1982).
[21] T. Riste, E. J. Samuelsen, and K. Otnes, Structural Phase Transitions and Soft Modes, edited by E. J. Samuelsen, E. Andersen, and J. Feder (Universitetsforlaget, Oslo, 1971), p. 395.
[22] T. Riste, E. J. Samuelsen, K. Otnes, and J. Feder, Solid State Commun. 9, 1455 (1971).
[23] N. C. Lagakos and H. Z. Cummins, Phys. Rev. B 10, 1963 (1974); E. Courtens and R. W. Gammon, Phys. Rev. B 24, 3890 (1981), and references cited in the paper.
[24] T. Yagi, H. Tanaka, and I. Tatsuzaki, Phys. Rev. Lett. 38, 609 (1977).
[25] S. M. Shapiro, J. D. Axe, G. Shirane, and T. Riste, Phys. Rev. B 6, 4332 (1972).
[26] M. D. Mermelstein and H. Z. Cummins, Phys. Rev. B 16, 2177 (1977).
[27] E. Courtens, Phys. Rev. Lett. 41, 1171 (1978).
[28] B. I. Halperin and C. M. Varma, Phys. Rev. B 14, 4030 (1976).
[29] For a recent review on this subject, see A. D. Bruce and R. A. Cowley, Adv. Phys. 29, 219 (1980).
[30] T. Schneider and E. Stoll, Phys. Rev. Lett. 31, 1254 (1975); 35, 296 (1976); Phys. Rev. B 17, 1302 (1980).
[31] C. P. Enz, Phys. Rev. B 6, 4695 (1972); E. Courtens and R. Gammon, Ferroelectrics 24, 19 (1980).
[32] G. J. Coombs and R. A. Cowley, J. Phys. C 6, 121 (1973).
[33] J. A. Krumhansl and J. R. Schrieffer, Phys. Rev. B 11, 3535 (1975).

[34]R. W. Gammon and H. Z. Cummins, Phys. Rev. Lett. **17**, 193 (1966).

[35]C. X. An, J. P. Benoit, G. Hauret, and J. P. Chapelle, Solid State Commun. **31**, 581 (1979).

[36]O. V. Kovalev, *Irreducible Representation of the Space Group* (Gordon and Breach, New York, 1965).

[37]E. M. Lifshitz and L. P. Pitaevski, *Statistical Physics—Part* 1,(Pergamon, New York, 1980).

[38]A. Yoshihara, W. D. Wilber, E. R. Bernstein, and J. C. Raich, J. Chem. Phys. **76**, 2064 (1982); A. Yoshihara, E. R. Bernstein, and J. C. Raich, *ibid.* **77**, 2768 (1982).

[39]A. Yoshihara, C. L. Pan, E. R. Bernstein, and J. C. Raich, J. Chem. Phys. **76**, 3218 (1982).

[40]A. Yoshihara and E. R. Bernstein, J. Chem. Phys. **77**, 5319 (1982).

[41]W. Yao, H. Z. Cummins, and R. H. Bruce, J. Chem. Phys. **24**, 424 (1981).

[42]F. Schwabl, Phys. Rev. B **7**, 2038 (1973).

[43]G. Hauret and J. P. Benoit, Ferroelectrics **40**, 1 (1982).

[44]Y. Tsujimi, T. Yagi, H. Yamashite, and I. Tatsuzaki, J. Phys. Soc. Jpn. **50**, 184 (1981).

[45]L. D. Landau and I. M. Khalatnikov, Dokl. Akad. Nauk, **96**, 469 (1954).

[46]J. C. Toledano, Phys. Rev. B **20**, 1147 (1979).

[47]H. Terauchi, T. Kojima, K. Sakaue, and F. Tajiri, J. Chem. Chem. Phys. **76**, 612 (1982).

[48]A. Yoshihara, E. R. Bernstein, and J. C. Raich, J. Chem. Phys. (submitted).